

Cyclic exchange, isolated states, and spinon deconfinement in an XXZ Heisenberg model on the checkerboard lattice

Nic Shannon,^{1,2} Grégoire Misguich,³ and Karlo Penc⁴

¹*Department of Advanced Materials Science, Graduate School of Frontier Sciences, University of Tokyo, 5-1-5, Kashiwahmoha, Kashiwa, Chiba 277-8851, Japan*

²*CREST, Japan Science and Technology Agency, Kawaguchi 332-0012, Japan*

³*Service de Physique Théorique, CEA-Saclay, 91191 Gif-sur-Yvette Cédex, France*

⁴*Research Institute for Theoretical Solid State Physics and Optics, H-1525 Budapest, P.O.B. 49, Hungary*

(Received 25 March 2004; published 10 June 2004)

The antiferromagnetic Ising model on a checkerboard lattice has an ice-like ground state manifold with extensive degeneracy. and, to leading order in J_{xy} , deconfined spinon excitations. We explore the role of cyclic exchange arising at order J_{xy}^2/J_z on the ice states and their associated spinon excitations. By mapping the original problem onto an equivalent quantum six-vertex model, we identify three different phases as a function of the chemical potential for flippable plaquettes—a phase with long range Néel order and confined spinon excitations, a nonmagnetic state of resonating square plaquettes, and a quasicollinear phase with gapped but deconfined spinon excitations. The relevance of the results to the square-lattice quantum dimer model is also discussed.

DOI: 10.1103/PhysRevB.69.220403

PACS number(s): 75.10.Jm, 64.60.Cn

The past decade has seen a great renaissance in the study of frustrated quantum spin systems. On the experimental front, advances in the synthesis of magnetic oxides have given rise to a great wealth of new frustrated materials with highly unusual and interesting properties. And, at the same time, highly frustrated models have become a favorite playground of theorists seeking to understand unconventional phase transitions and excitations.

Recently, it was proposed that the geometric frustration present on the pyrochlore lattice could give rise to fractional charges in two or three dimensions,¹ in a physically realistic model based on strong nearest neighbor repulsion close to commensurate filling.² The charge ordering problem considered in Ref. 1 is classically equivalent to one of Ising antiferromagnetism, and in this paper we consider the simplest possible test case for these ideas, the XXZ Heisenberg model on a checkerboard (2D pyrochlore) lattice. We proceed by mapping this model onto an equivalent, quantum six-vertex model (Q6VM), and describe the nature of the ground state and low lying spin excitations of this model as a function of a control parameter V , which acts as a chemical potential for those “flippable plaquettes” accessible to cyclic exchange.

We identify three different ground states, a phase with long range Néel order, a nonmagnetic state of resonating square plaquettes, and a partially disordered phase of “isolated states” with extremely large ground state degeneracy, referred to as the “quasicollinear” phase below. Because of the anisotropy of the model, all spin excitations are gapped. It is possible to identify the lowest lying excitations of the Néel phase as spin waves, and those of the quasicollinear phase as deconfined spinons. We also identify the special role of the isolated states in supporting fractional excitations. Many of these results are also relevant to the much studied square lattice quantum dimer model (QDM).³

Model and mapping onto Q6VM: We take as a starting point the spin-1/2 anisotropic Heisenberg model with anti-

ferromagnetic interactions, $J_z, J_{xy} > 0$, in the limit $J_z \gg J_{xy}$

$$\mathcal{H} = J_z \sum_{\langle ij \rangle} S_i^z S_j^z + \frac{J_{xy}}{2} \sum_{\langle ij \rangle} (S_i^+ S_j^- + S_i^- S_j^+). \quad (1)$$

Here the sum $\sum_{\langle ij \rangle}$ runs over the bonds of the 2D pyrochlore or checkerboard lattice, shown in Fig. 1(a). In the Ising limit, $J_{xy}=0$, this model has an extensive ground state degeneracy—every state with exactly two up and two down spins per tetrahedron (cross linked square) is a ground state. For historical reasons, this is known as the “ice rules” constraint. Topologically, “ice” states have the structure of closely packed loops of up and down spins, and are separated by a gap J_z from the lowest lying excited state. Flipping any

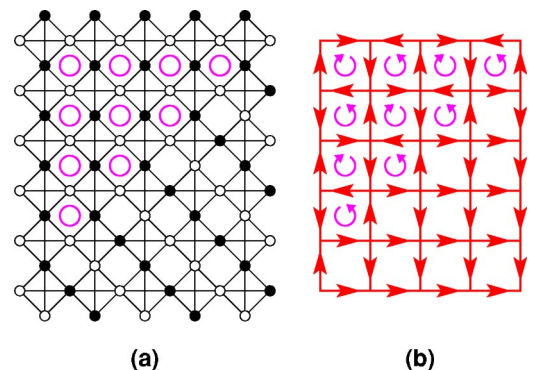


FIG. 1. (Color online) (a) The checkerboard lattice on which the ice states, and (b) the square lattice on which the states of the six-vertex model are defined. Any Ising state obeying the ice rules, e.g., that shown in (a), is equivalent to (b) six-vertex model configuration. In the state shown, the upper left corner has Néel order, while the lower right corner has collinear order. Flippable plaquettes are denoted with circles. In the case of the six-vertex model, these have a definite sense of rotation.

given down spin connects two adjacent loops of up spins, creating two “ T -junction” like topological defects (spinons), which propagate independently.^{1,4} The pyrochlore (checkerboard) lattice is bipartite in tetrahedra. Spinons are created in A and B sublattice pairs, and move so as to preserve tetrahedron sublattice.

By drawing an arrow from the center of A to B sublattice tetrahedra where they share an up spin, and from B to A where they share a down spin, one can show that the many ground states of the Ising model on a checkerboard lattice are in exact, one-to-one correspondence with the states of the classical *six vertex model* (6VM),^{5,6} widely studied as a 2D analog of water ice. From this mapping, we know that (a) the ground state manifold of the Ising model grows as $W \propto (4/3)^{3N/4}$ where N is the number lattice sites⁷ and (b) all correlation functions decay algebraically.⁸

Up to this point, our analysis contains only classical statistical mechanics and simple topological arguments. Quantum mechanics reenters the problem when we consider a small but finite $J_{xy} \ll J_z$. In this case, the ice states are no longer eigenstates. Short lived virtual excitations enable the system to tunnel between different ice state configurations wherever pairs of upspins and downspins occur diagonally opposite one another on one of the empty square plaquettes of the checkerboard lattice.⁹ The allowed reconfigurations of these “flippable plaquettes” can be described within degenerate perturbation theory by the effective Hamiltonian

$$\mathcal{H}_{2\text{nd}} = -\frac{J_{xy}^2}{J_z} \sum_{\square} (S_1^+ S_2^- S_3^+ S_4^- + S_1^- S_2^+ S_3^- S_4^+), \quad (2)$$

where the indices 1–4 count consecutive sites (either clockwise or anticlockwise), of an empty plaquette.⁶

In terms of the 6VM representation, Eq. (2) acts on a plaquette where four arrows are joined nose to tail, so as to invert all of the arrows and change the sense of rotation of the plaquette (cf. Ref. 10). The quantum dynamics in the Q6VM we consider are directly analogous to the resonance of dimers in the QDM,³ studied as a simplified model of a resonating valence bond state.¹¹ Formally, in fact, the Hamiltonian is exactly the same, although the Hilbert space on which it acts is different. And, as in the QDM, we anticipate that quantum effects will in general select a ground state with finite degeneracy from the vast manifold of classically allowed ice states.

As such, there is only one (kinetic) energy scale in the problem, $t = J_{xy}^2 / J_z$. However in order to study the different possible phases of the model it is useful to introduce a further control parameter. A suitable control parameter for the QDM is a diagonal term which counts the number of dimers which can resonate in any given dimer covering. By direct analogy, we introduce a diagonal interaction V to the Q6VM which counts the number of flippable plaquettes

$$\mathcal{H} = \sum_{\square} [V(|\circlearrowleft\rangle\langle\circlearrowleft| + |\circlearrowright\rangle\langle\circlearrowright|) - t(|\circlearrowleft\rangle\langle\circlearrowright| + |\circlearrowright\rangle\langle\circlearrowleft|)], \quad (3)$$

where the $|\circlearrowleft\rangle$ and $|\circlearrowright\rangle$ states represent squares with the respective circular arrow configuration on the square edges,

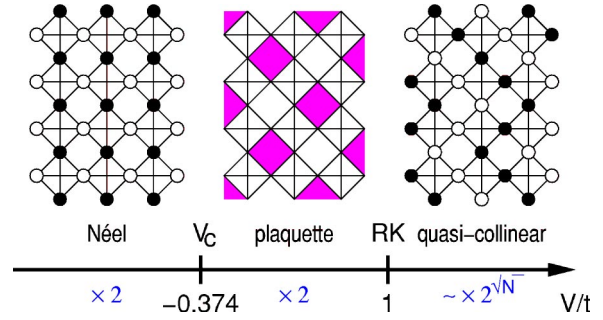


FIG. 2. (Color online) The phase diagram of the model as a function of V/t . The Néel phase breaks the point group, while the plaquette phase breaks the translational symmetry. The Rokhsar-Kivelson point is marked RK.

as seen in Fig. 1(b). We note that, for a system with periodic boundary conditions, the net flux of vertex arrows through any given horizontal or vertical cut defines a set of winding numbers which are conserved by the Hamiltonian (3).

Our approach to determining the different phases of the Hamiltonian (3) is the numerical diagonalization of clusters with periodic boundary conditions of up to 64 spins, within the ice rules manifold of states, supplemented with topological and symmetry arguments. Details of these, together with further analysis of the related fermionic charge-ordering problem will be discussed further in separate publications.^{12,13}

Phase diagram: We first consider the nature of the ground state as a function the chemical potential for flippable plaquettes, V . Our results are summarized in the phase diagram Fig. 2, and the numerical evidence for each phase discussed below.

Negative values of V favor states with flippable plaquettes. The state with the greatest possible number of flippable plaquettes is the Néel state, and this must be the ground state for $V \rightarrow -\infty$. The Néel state is twofold degenerate in the thermodynamic limit. For finite V/t , in a finite size system, quantum fluctuations lift this degeneracy, as seen in the low-energy spectrum of the Q6VM (Fig. 3). We find a single phase for $V \leq -0.3t$, which we identify as the Néel phase. Both the symmetric and antisymmetric combinations of the two symmetry-breaking Néel ground states are visible in the spectrum, marked “GS” and “Néel,” respectively. At a value of $V \sim -0.3t$, a third energy level, marked “Plaq” crosses the first excitation “Néel.” We interpret this as evidence for a quantum phase transition into a resonating plaquette phase, discussed below. From finite size scaling of the spectrum (Fig. 4) we estimate the critical value to be $V_c = -0.3727t$ in the thermodynamic limit. As the competing Néel and plaquette order parameters break lattice symmetries in very different ways, the transition between them is presumably of first order.

We find a single phase extending from $-0.3t \leq V \leq t$, including the XXZ point $V=0$. This phase terminates in the special high symmetry point $V=t$ for which the Hamiltonian (3) of the Q6VM can be written as a sum of projection operators:

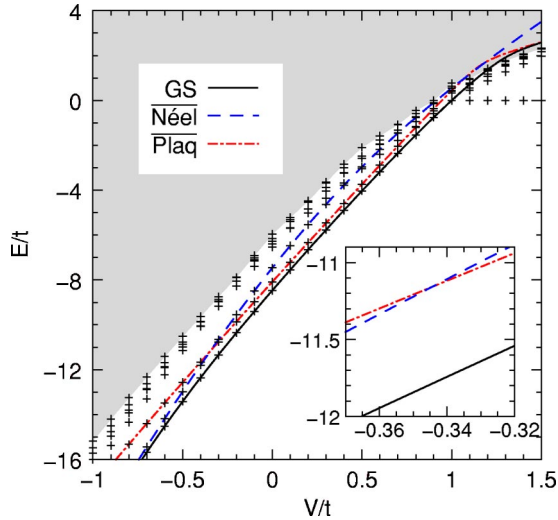


FIG. 3. (Color online) Energy level diagram of the 32-site pyrochlore-slab with periodic boundary conditions as a function of V/t , obtained by numerical diagonalization. We have shown the first eight levels. Inset: the first two excited states cross at $V_c/t = -0.3437$ (the axes are the same as of the main plot).

$$\mathcal{H}_{\text{RK}} = t \sum_{\square} (|\odot\rangle - |\ominus\rangle)(\langle\odot| - \langle\ominus|). \quad (4)$$

Following Rokhsar and Kivelson (RK),³ we can construct a zero eigenvalue state of the \mathcal{H}_{RK} by taking the linear combination of all the states in a given topological sector with the same amplitude. Since this state is annihilated by the positive semidefinite \mathcal{H}_{RK} , it must be a ground state. As in the QDM, static correlations can be computed exactly at this point. Like the correlation functions of the 6VM, they decay algebraically with distance.

At the RK point, kinetic, and potential energy are perfectly balanced; in the plaquette phase kinetic energy dominates, and resonating plaquettes repel one another so as gain the maximum kinetic energy.¹⁴ The resulting state is essentially a Peierls-like distortion of the RK state in which only A (B) sublattice plaquettes resonate $\Pi_{\square_{A(B)}}(|\odot\rangle + |\ominus\rangle)$. The

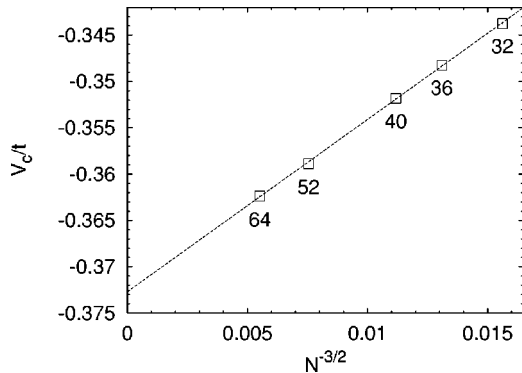


FIG. 4. Estimate of the phase boundary between the Néel and plaquette phases. Empirically, the values of V_c where the level crossings occur scale as $-0.3727 + 1.86N^{-3/2}$. Values are shown for 32, 36, 40, 52, and 64 pyrochlore-slab sites.

way in which the phase breaks lattice symmetries—it is two-fold degenerate, and invariant under operations which map the alternating A and B plaquette sublattice onto themselves—suggest the plaquette phase of the Q6VM is an Ising analog of the SU(2) valence-bond crystal of resonating plaquettes. Such a phase has been proposed in the context of the square lattice QDM.¹⁵ Furthermore, the ground state of the Heisenberg-model on a checkerboard lattice is a valence bond crystal of SU(2) singlets formed on alternate empty plaquettes,¹⁶ with a possibility of an adiabatic continuity between the ground state of the XXZ and SU(2) symmetric Heisenberg models.¹⁷

For $V > t$ the ground state is the highly degenerate manifold of “isolated” states with no flippable plaquettes. They are eigenstates with 0 energy for any value of V/t , and become the ground state for $V > t$.¹⁸ The prototype of an isolated state is the collinear configuration shown in Fig. 1. In this reference state all vertex arrows point from left to right or from top to bottom. Inverting the direction of the arrows along an arbitrary number of lines, subject to the constraint that all of them are either horizontal or vertical, creates new isolated states. This leads to a ground state degeneracy which grows as $4(2^p - 1)$ for regularly shaped clusters, where $p \sim \sqrt{N}$. In these states, the direction of arrows along either the horizontal or vertical lines is long-range ordered, but quantum effects none the less fail to select a ground state with finite degeneracy. We refer to this phase of the Q6VM as “quasicollinear.” Finally, since the transition between the quasicollinear phase and the resonating plaquette phase takes place through the softening of specific excitation (discussed below), we identify it as second order.

Excitations: First let us consider the nature of excitations at fixed $S^z = 0$. A state with n flippable plaquettes has a diagonal matrix element nV and is connected to n other states. Gerschgorin’s theorem places a bound $|H_{ii} - \varepsilon_i| < \sum_j |H_{ij}|$ on the separation of the i th eigenvalue ε_i from the diagonal matrix element H_{ii} . In the case in point, this bound is $|nV - \varepsilon_i| < nt$, or $n(V-t) < \varepsilon_i < n(V+t)$. The smallest energy in an arbitrary topological sector is thus larger than $V-t$, which gives a lower bound on the value of the gap in the quasicollinear phase for $V > t$. This above argument permits a gapless spectrum at the RK point $V=t$. In fact it is possible to explicitly construct a family of states with a gap that vanishes at the RK point, as shown in Fig. 5(a): the energy spectrum of this particular excitation forms a continuum between $2V - 2t$ and $2V + 2t$.

Now let us consider spin excitations with $S^z = \pm 1$. If we neglect virtual processes at order J_{xy}^2/J_z , and the possibility of entropic confinement at finite temperature, these propagate as independent fractional excitations.¹ Quantum effects may, or may not, act to confine these excitations, depending on the type of correlations present in the ground state they select. The Néel ground state has a twofold ground state degeneracy, and separating the topological defects created by flipping a spin creates a string of unflippable plaquettes. This leads to confinement of spinons, and the low lying spin excitations of the Néel phase of our model have the same quantum numbers as a spin wave. On general grounds, we expect the same to be true of the plaquette phase.

The manifold of isolated states selected by V can support

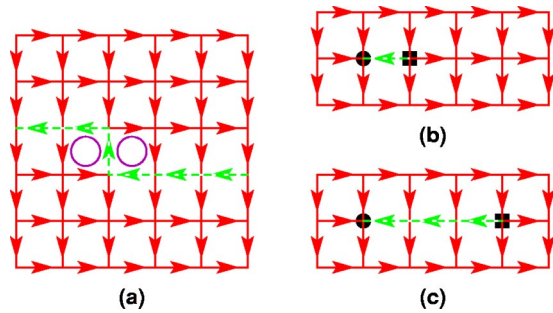


FIG. 5. (Color online) (a) A “leapfrog” excitation in the quasi-collinear phase. Two flippable plaquettes (denoted with circles) are created by reversing the arrows of the collinear reference state on a line with a single one-step kink. The motion of the pair of flippable plaquettes is equivalent to a one-dimensional hopping model with an energy spectrum $\varepsilon(k)=2V+2t \cos k$, where k is an effective one-dimensional momentum. (b) and (c): The deconfined spinons in the collinear phase (black dots). Note, that spinons hop so as to stay within a given sublattice of the (bipartite) square lattice.

deconfined spinons, however. Since no new flippable plaquettes are introduced into isolated states by flipping a single spin, and the pair of topological defects created by flipping a single spin can be separated without creating new flippable plaquettes, spinons are deconfined. An example of a pair of deconfined spinon excitations is shown in Figs. 5(b) and 5(c). For $V \gg J_{xy} \gg t$, spinon motion is movement is con-

finned to the x and y directions, but by scattering off one another, a pair of spinons can explore the full two dimensional space of the lattice. Whether a more general class of deconfined spinon excitation becomes possible as one approaches the RK point remains an open question. We also note that while fixing the boundary conditions will lift the degeneracy of the isolated state manifold, it need not affect the arguments for spinon deconfinement presented above.

Conclusions: We have established that, as a function of the chemical potential for “flippable plaquettes” accessible to cyclic exchange, the XXZ Heisenberg model on a checkerboard lattice exhibits Néel, resonating plaquette and quasi-collinear phases. If virtual processes at J_{xy}^2/J_z are ignored, spinon excitations in the XXZ Heisenberg model are deconfined. We have shown explicitly that a subset of spinon excitations—those associated with isolated states—remain deconfined even when these quantum effects are taken into account. Finally, we mention that the equivalents of both the “leap-frog” and spinon excitations can also be constructed in the square-lattice QDM for $V > t$.¹⁹

The authors are pleased to acknowledge helpful discussions with P. Fazekas, P. Fulde, R. Moessner, V. Pasquier, E. Runge, D. Serban, A. Sütő, M. Roger, P. Sindzingre, and P. Wiegmann. We thank the support of the Hungarian OTKA T038162 and T037451, EU RTN “He III Neutrons” and the guest program of MPI-PKS Dresden.

¹P. Fulde, K. Penc, and N. Shannon, *Ann. Phys. (Leipzig)* **11**, 892 (2002).

²P. W. Anderson, *Phys. Rev.* **102**, 1008 (1956).

³D. S. Rokhsar and S. A. Kivelson, *Phys. Rev. Lett.* **61**, 2376 (1988).

⁴M. Hermele and M. P. A. Fisher, and L. Balents, *Phys. Rev. B* **69**, 064404 (2004).

⁵J. Kohanoff, G. Jug, and E. Tosatti, *J. Phys. A* **23**, L209 (1990); R. Moessner and S. L. Sondhi, *Phys. Rev. B* **63**, 224401 (2001).

⁶R. Moessner, O. Tchernyshyov, and S. L. Sondhi, cond-mat/0106286 (unpublished).

⁷E. Lieb, *Phys. Rev. Lett.* **18**, 692 (1967).

⁸R. Baxter, *Exactly Solved Models in Statistical Mechanics* (Academic, San Diego, 1982), pp. 127–179.

⁹This is in marked contrast to the XXZ model on a triangular lattice, where the states in the ground-state manifold are connected directly by J_{xy} , leading to the RVB picture in P. Fazekas and P. W. Anderson, *Philos. Mag.* **30**, 423, (1974).

¹⁰S. Chakravarty, *Phys. Rev. B* **66**, 224505 (2002).

¹¹P. W. Anderson, *Mater. Res. Bull.* **8**, 153 (1973).

¹²K. Penc and N. Shannon (unpublished).

¹³E. Runge and P. Fulde (unpublished).

¹⁴The plaquette phase has also recently been observed in Quantum Monte Carlo simulations; R. Moessner (private communication).

¹⁵P. W. Leung, K. C. Chiu, and K. J. Runge, *Phys. Rev. B* **54**, 12938 (1996).

¹⁶P. Sindzingre, J.-B. Fouet, and C. Lhuillier, *Phys. Rev. B* **66**, 174424 (2002), and references therein.

¹⁷Further numerical work confirms this conjecture; P. Sindzingre (private communication).

¹⁸The (non)existence of isolated states is intimately related to the nature of the ground state, see, e.g., A. Sütő, *Z. Phys. B: Condens. Matter* **44**, 121 (1981).

¹⁹The similarity between the two models can be traced back to the lattice bipartiteness and the existence of a common height representation for both the dimer coverings [H. W. J. Blote and H. J. Hilhorst, *J. Phys. A* **15**, L631 (1982)] and 6 VM states (Ref. 5), where isolated states are those with a maximum “tilt.”